

# A power amplifier for a femtosecond terawatt Cr : forsterite laser system

A.V. Ovchinnikov, S.I. Ashitkov, M.B. Agranat, D.S. Sitnikov

**Abstract.** A three-stage power amplifier is developed for an IR terawatt femtosecond laser system generating 80-fs, 1240-nm pulses with energy of up to 90 mJ, a pulse repetition rate 10 Hz, and the intensity contrast above  $10^6$ . The efficiencies of different schemes of multipass amplifiers are compared. It is shown that an optical scheme with plane mirrors is optimal for achieving the terawatt power level.

**Keywords:** Cr : forsterite, amplification of femtosecond pulses, terawatt laser system.

We reported earlier [1] the development of a terawatt Cr : forsterite laser system based on the chirped pulse amplification (CPA) principle [2, 3]. The system consisted of a master oscillator, a stretcher, a preamplifier based on a ring regenerative amplifier (RA) [4], a four-stage power amplifier, and a compressor and generated 80-fs, 90-mJ pulses at a wavelength of 1240 nm with a pulse repetition rate of 10 Hz. Other CPA Cr : forsterite systems [5, 6] known to us before the fabrication of our laser system used only a RA and emitted pulsed energies only up to 0.8 mJ [6].

In this paper, we present the results of studies of several schemes of Cr : forsterite multipass amplifiers (MPAs). We modernised a power amplifier described in [1]. Due to the increase in the gain achieved by using two-sided pumping and optimising the length of crystals, the number of transits and amplification stages was decreased. The contrast of output pulses of the terawatt femtosecond laser system was measured by using a third harmonic correlator.

Because the pulse energy of a femtosecond Cr : forsterite crystal does not exceed a few nanojoules, the energy amplification by  $10^7 - 10^8$  times is needed to generate terawatt pulses. Such a high gain is achieved by using RAs and MPAs. The main difficulty is that the intensity of directly amplified femtosecond pulses achieves the nonlinear threshold already at energies of the order of a few microjoules. To avoid this, the CPA method [2, 3] is used in which the output pulse of a master oscillator is transmitted

through a delay line with a high group velocity dispersion (a stretcher), which results in the increase in the pulse duration by  $10^3 - 10^4$  times. After amplification, the pulse is again transmitted through a delay line having the same group velocity dispersion but with the opposite sign. As a result, the pulse is compressed to acquire the duration close to its initial value (before the stretcher).

The optical scheme of the femtosecond Cr : forsterite laser system is presented in Fig. 1.

Femtosecond pulses were generated by a master oscillator with a Z-type resonator [7] which had an average output power of  $\sim 200$  mW at a wavelength of 1250 nm with the 50-nm full width at half-maximum (FWHM). The output pulse energy achieved 2.3 nJ. The stretcher used a scheme with one diffraction grating, which provided the increase in the pulse duration by a factor of  $10^3$ . The stretcher efficiency (the intensity ratio of the output and input pulses) was  $\sim 60\%$ .

The maximum amplification of laser pulses is usually achieved in the first stage operating in the small-signal gain regime. In terawatt Ti : sapphire systems, where the energy ratio of the output and input pulses per pass in the active medium achieves 8, due to their high gain both regenerative and multipass schemes are used as a preamplifier. The gain in a Cr : forsterite crystal is much lower (no more than 2 per pass), and therefore regenerative schemes providing a great number (a few tens) of transits are more efficient for using at the first stage.

We used in our scheme a RA with a ring resonator. The advantage of this scheme compared to the widely used linear scheme is the absence of an optical isolator (usually a Faraday cell) between the amplifier and master oscillator. The contrast of the output radiation of a ring RA is twice that of a RA with a linear resonator [8]. The operation and basic parameters of the RA are described in detail in [4]. Here we present only the main output parameters. The bandwidth (FWHM) of the output radiation from the RA was 26 nm and the central wavelength was shifted to the blue by 20 nm with respect to the master oscillator wavelength. The maximum gain of a pulse was achieved after 46–48 transits in the active medium, and then the pulse was coupled out of the resonator with the help of a controllable Pockels cell. The pulse energy was increased in this case from 1.4 nJ to 400  $\mu$ J, which corresponds to the gain  $3 \times 10^5$ . The intensity contrast between the main separated pulse and the prepulses emerging from the RA was  $\sim 10^3$ .

To provide a higher contrast, which is required for the efficient amplification of a single pulse in an MPA, we used the scheme consisting of two crossed polarisers (Glan

A.V. Ovchinnikov, S.I. Ashitkov, M.B. Agranat, D.S. Sitnikov Joint Institute for High Temperatures, Russian Academy of Sciences, ul. Izhorskaya 13/19, 125412 Moscow, Russia;  
e-mail: ashitkov11@yandex.ru

Received 29 August 2007

Kvantovaya Elektronika 38 (4) 325–329 (2008)

Translated by M.N. Sapozhnikov

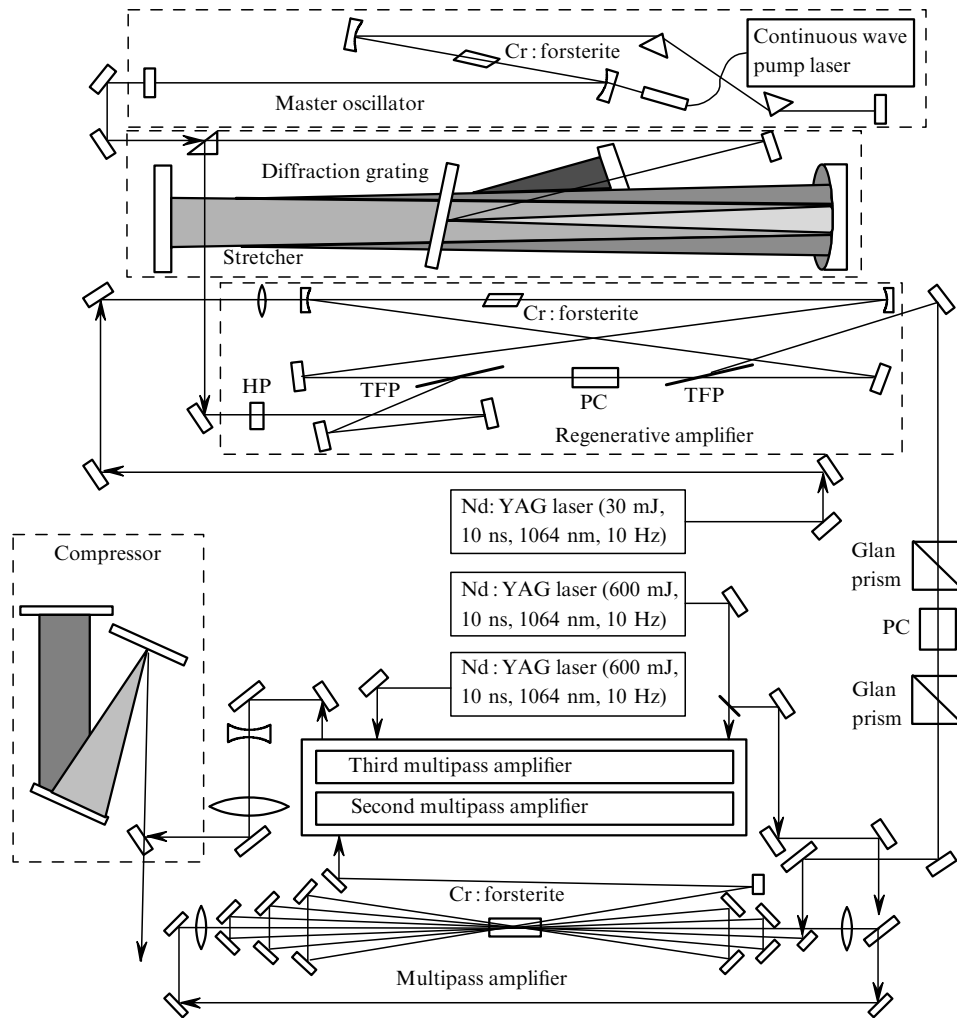


Figure 1. Optical scheme of the femtosecond Cr : forsterite laser system: (TFP) thin-film polariser; (PC) Pockels cell; (HP) half-wave plate.

prisms) and another Pockels cell located between them. This cell was controlled by the 10-ns electric pulse, which was synchronised with a pulse controlling the Pockels cell mounted in the RA. This scheme improved the intensity contrast between the main pulse and prepulses almost by three orders of magnitude, which is important in experiments with high-power femtosecond radiation because prepulses should not produce any changes at the target surface before the action of the main pulse. In addition, these prepulses, passing through the end amplification stages, reduce the population inversion, which decreases their efficiency.

In the development of a MPA, we studied the parameters of two optical schemes. One of them (Fig. 2) consisted of two spherical mirrors with different radii of curvature (with holes at the centre) forming a confocal resonator, and of an active element placed at the focus of these mirrors. A similar optical scheme with a typical number of transits 4–8 [9] is widely used instead of RAs in high-power femtosecond Ti:sapphire lasers. Its main advantages are compactness and a small number of optical elements. A small size of the amplified signal mode focused into a crystal provides a high gain at low pump levels. However, amplification rapidly saturates for this reason, which is the main disadvantage of this scheme.

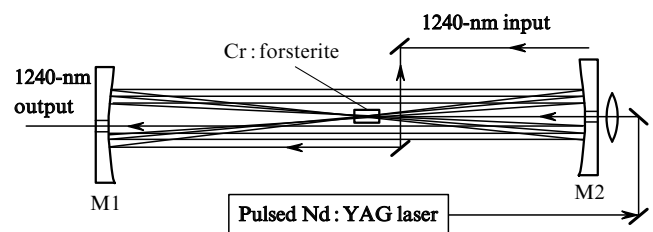
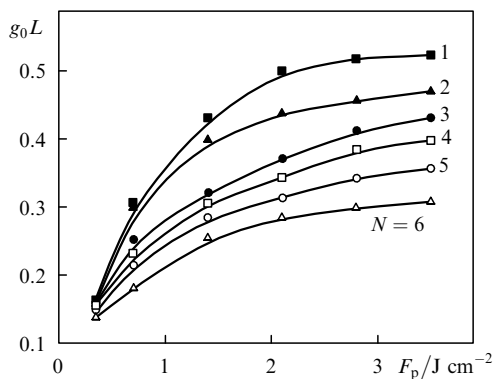


Figure 2. Multipass amplifier with spherical mirrors M1 and M2.

We used a scheme with six transits of a laser pulse through the active element. The radii of curvature of mirrors M1 and M2 were 1100 and 900 mm, respectively. The amplifier had the optical scheme of a telescope. The radiation spot size on mirror M1 decreased after each round trip in the amplifier, while the beam diameter inside the crystal increased. As a result, the mode size (hereafter, at the  $e^{-1}$  level) increased from 0.4 mm after the first round-trip transit up to 1.2 mm after the six transit. Radiation approached the optical axis of the amplifier after six round trips and was coupled out of the amplifier through the hole in mirror M1. The crystal was cut at the Brewster angle and

had dimensions 11, 3, and 3 mm along the crystallographic axes  $a$ ,  $b$ , and  $c$ , respectively. The pump beam was directed along the  $a$  axis, and the polarisation vector was directed along the  $b$  axis. Pumping was performed by a  $Q$ -switched Nd:YAG laser. The 1064-nm, 100-mJ pump pulses were focused to the crystal by a lens with a focal distance of 500 mm through the hole in mirror M2. Before focusing, the pump radiation passed through an attenuator consisting of a half-wave plate and a film polariser, which provided the control of energy and, hence, the energy density of the pump pulse in the active element. The pump mode size in the crystal was about 1.5 mm at the maximum energy density of  $3.5 \text{ J cm}^{-2}$ . A further increase in the pump energy density did not enhance the gain (Fig. 3) because the excited state absorption (ESA) increased [6]. In this case, about 70 % of the pump pulse energy was absorbed in the crystal.



**Figure 3.** Dependence of the MPA gain  $g_0L$  on the pump energy density  $F_p$  for different transits;  $N$  is the transit number.

The small-signal gain in the active medium of the amplifier is described by the expression

$$I_{\text{out}} = I_{\text{in}} \exp[(g_0 - \alpha)L], \quad (1)$$

where  $I_{\text{in}}$  and  $I_{\text{out}}$  are the input and output radiation intensities of the active element;  $L$  is its length; and  $g_0$  and  $\alpha$  are the gain and absorption coefficients. The absorption coefficient  $\alpha$  measured after the propagation of a weak signal in the active medium in the absence of pumping was  $\sim 0.15 \text{ cm}^{-1}$  ( $\sim 7\%$  per pass in the crystal of length 11 mm). Figure 3 shows the experimental dependences of  $g_0L$  at a wavelength of 1240 nm on the pump energy density for different transits in the active element of the amplifier. One can see that the gain gradually decreases with increasing the transit number due to the decrease in the excited-state population.

The dependence of the output pulse energy of the MPA on the input pulse energy is shown in Fig. 4. One can see that when the input pulse energy achieves 300  $\mu\text{J}$ , the output pulse energy begins to saturate, i.e. it almost ceases to increase because the population inversion is insufficient for obtaining the output energy exceeding 2.3 mJ. When the input pulse energy exceeds 300  $\mu\text{J}$ , the maximum output pulse energy is achieved after a smaller number of transits, but does not exceed this value. The amplifier efficiency, i.e. the ratio of the difference of the output and input pulse energies to the pump pulse energy was 6 %.

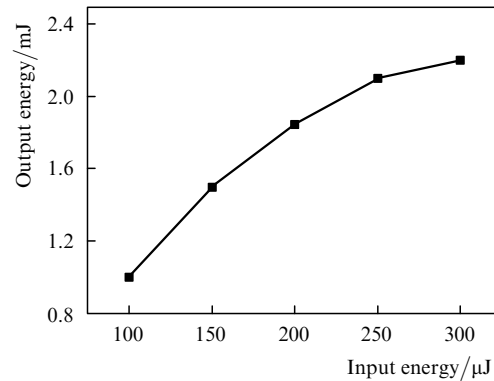


**Figure 4.** Dependence of the MPA output pulse energy on the input pulse energy.

The analysis of our data showed that, to increase the maximum output pulse energy, it is necessary to increase the pump mode diameter in the active medium and to increase the size of the amplified signal mode, i.e. to produce a large volume of the inverted active region. However, the optical system considered above cannot provide variations in the size of the amplified signal within the required limits. Because of this, we tested another MPA scheme with plane mirrors (Fig. 5) [10]. The active medium was a cylindrical Cr:forsterite crystal of size  $\varnothing 6.3 \times 21 \text{ mm}$  with AR-coated end-faces (at 1240 nm). The figure of merit of the crystal was 25, and the crystal absorbed  $\sim 85\%$  of the pump radiation.

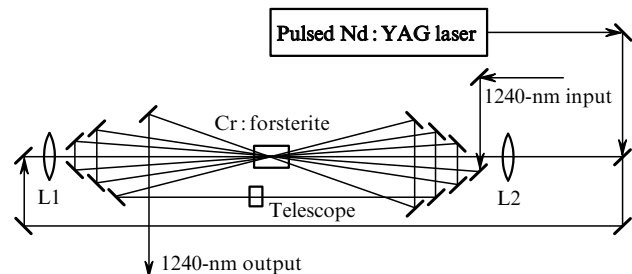


**Figure 5.** Optical scheme of the MPA with plane mirrors: L1 and L2 are focusing lenses.

The pump pulse parameters were similar to those presented above. The mode diameter was 2 mm for the energy density  $3\text{--}3.5 \text{ J cm}^{-2}$ . Because the diameter of the RA output beam was  $\sim 1 \text{ mm}$ , a  $2\times$  telescope was used to match the amplified signal mode with the pump mode diameter. This telescope also compensated for a thermal lens produced in the active element by absorbed pump radiation. The maximum small-signal gain per pass was measured to be 1.65. In this case, the output pulse energy was 4.5 mJ upon pumping by the  $3.2 \text{ J cm}^{-2}$  pulse.

An important disadvantage of the amplifier in which the active medium is pumped from one side is the nonuniformity of the population inversion resulting in the nonuniformity of amplification along the radiation propagation direction. According to the Bouguer law, the energy density  $F(z)$  of the pump pulse propagating along the  $z$  axis in a crystal decreases exponentially as

$$F(z) = F_p \exp(-\alpha z), \quad (2)$$

where  $F_p$  is the pump pulse energy density on the input surface of the active element.

Figure 6 shows the change in the pump energy density  $F$  along the  $z$  axis for the absorption coefficient equal to  $0.84 \text{ cm}^{-1}$ . Curves (1), (2), and (3) correspond to the pumping of the active element through its left and right end-faces, and simultaneously through both end-faces, respectively. It is easy to verify that upon pumping the active element through one of the end-faces, the pump energy density decreases by half already at a distance of 10 mm from this end-face. A more uniform distribution of the population inversion along the crystal can be obtained by pumping the crystal from two sides. In this case, the nonuniformity of the pump pulse energy density does not exceed 30% [curve (3) in Fig. 6]. The dependence of the gain on the pump energy density  $F_p$  during the first transit through the active element corresponding to this geometry is shown in Fig. 7 [curve (1)]. One can see that such pumping leads to the increase in the maximum gain by a factor of  $\sim 1.3$  compared to the case of pumping the active element from one side [curve (2) in Fig. 7]. The total gain of the MPA after six transits increased from 15 to 22, while the output pulse energy increased from 4.5 to 6.7 mJ. Because the total absorbed pump energy increased, the output energy density  $3\text{--}3.5 \text{ J cm}^{-2}$  was achieved at lower pump pulse energies from each side of the crystal than upon pumping from one side. Although the efficiency of the amplifying stage, as in the scheme with spherical mirrors,

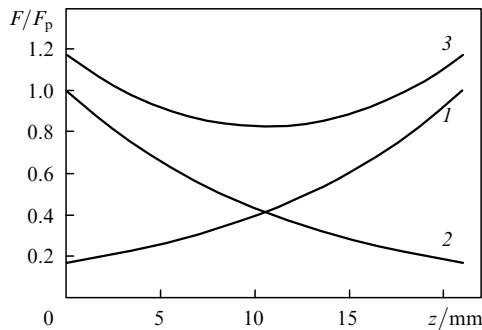


**Figure 6.** Dependences of the normalised pump energy density on  $z$  (along the active element) for  $L = 21 \text{ mm}$  upon pumping the crystal from one (1) and the other (2) side, and simultaneously from two sides (3).

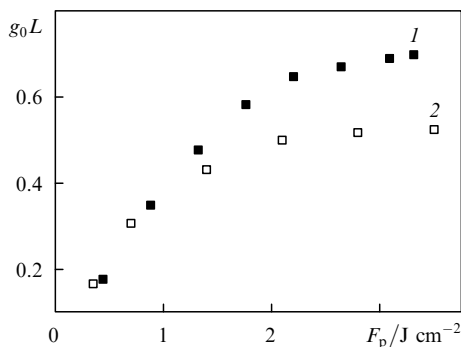


**Figure 7.** Dependences of the gain in active elements on the pump pulse energy density at the first transit upon pumping the active element from two sides (1) and from one side (2).

was about 6%, the maximum output pulse energy was higher in this case.

To obtain the output pulse energy  $\sim 100 \text{ mJ}$ , it is necessary to amplify the input pulse by a factor of 15. This was achieved by using two additional MPAs and the second pump laser. One of the lasers was used to pump the first and second amplifying stages and the other – to pump the third stage (see Fig. 1). To optimise the operation regime of amplifiers, we tested several Cr : forsterite active elements of different lengths differently absorbing the pump radiation (Fig. 8). These elements were pumped from two sides.

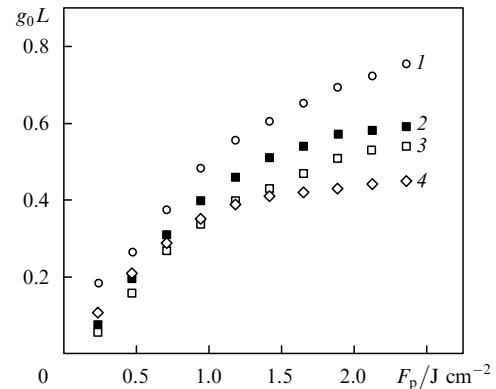


**Figure 8.** Dependences of the gain in active elements on the pump pulse energy at the first transit for absorption coefficients  $\alpha = 1.2 \text{ cm}^{-1}$  ( $L = 20 \text{ mm}$ ) (1),  $0.8 \text{ cm}^{-1}$  (24 mm) (2),  $0.8 \text{ cm}^{-1}$  (21 mm) (3), and  $1.2 \text{ cm}^{-1}$  (15 mm) (4).

The measurements show that the maximum amplification was achieved in the element of length 20 mm with the absorption coefficient for pump radiation equal to  $1.2 \text{ cm}^{-1}$ . This element was used in the second amplification stage. The element of length 24 mm with the absorption coefficient of  $1 \text{ cm}^{-1}$  had a slightly lower gain and was used in the third MPA stage.

The scheme of the second stage was similar to that of the first stage (Fig. 5), but used four transits. Behind the first stage, a  $2.5\times$  telescope was placed which provided the output pulse energy density of the second MPA  $\sim 0.5 \text{ J cm}^{-2}$  and also corrected the divergence of the input beam taking a thermal lens into account. The crystal surfaces also had AR coatings for a wavelength of 1240 nm. The optimal number of transits was determined by obtaining the maximum efficiency of conversion of the absorbed pump energy to the amplified signal energy. This maximum in the second stage was 12% for the pump pulse fluence on crystals faces equal to  $2.3 \text{ J cm}^{-2}$ . In this case, the output pulse energy of the MPA achieved 56 mJ. The output pulse energy after the similar third amplification stage was 115 mJ at the stage efficiency of 9%. A lower efficiency in this case is explained by the fact that the element used in this stage had a lower gain per pass (see Fig. 8) than in the second stage and also by the complexity of realising the third transit.

The amplified chirped pulse was compressed in a time compressor assembled in the optical scheme with two 600-lines  $\text{mm}^{-1}$  diffraction gratings of size  $100 \times 120 \text{ mm}$ . A  $3\times$  telescope placed in front of the compressor limited the energy density on diffraction gratings by the value  $100 \text{ mJ cm}^{-2}$ . The compressor was tuned to the minimal

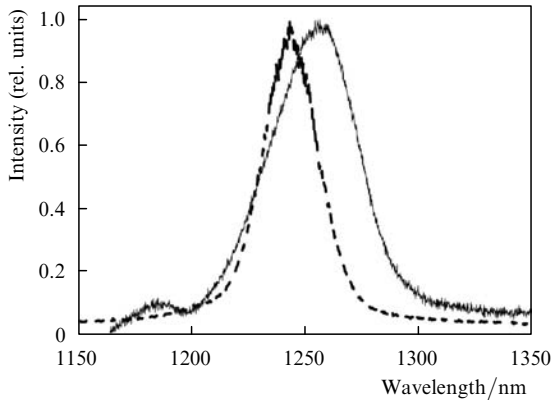


**Figure 9.** Spectra of the output pulse of the master oscillator (solid curve) and the output pulse of the terawatt laser system (dashed curve).

pulse duration by varying the distance between the gratings. The compressor efficiency was 77 % for the 90-mJ output femtosecond pulse energy.

Figure 9 shows the emission spectra of the master oscillator and the output pulse (at the terawatt power level). The FWHM of the emission spectrum of the master oscillator was  $\sim 50$  nm and that of the output pulse of the system was  $\sim 30$  nm, which corresponds to the  $\sim 80$ -fs duration of the output pulse.

In experiments with high-power femtosecond pulses, not only the pulse duration is important but also its temporal profile. The latter was studied by using a correlator with the dynamic range of signal detection up to  $10^9$ . The operation principle of this correlator is based on the measurement of the third-order cross-correlation function. The correlator provided the measurement of the background caused by the amplified spontaneous emission (ASE) and also the recording of prepulses and postpulses [11]. The typical cross-correlation function is presented in Fig. 10. One can see that the intensity contrast achieved in the system is no less than  $10^4$  for 1 ps and more than  $10^6$  for 2 ps before the pulse maximum.

The instability of the output pulse energy of the terawatt Cr : forsterite system was mainly determined by the instability of the pump pulse energy and did not exceed  $\sim 5$ %.

Note in conclusion that the possibility of obtaining the high energy efficiency in power amplifiers pumped by lasers

at 1064 nm makes promising the use of Cr:forsterite crystals as active media for femtosecond terawatt IR laser systems. The lower gain compared to that in Ti:sapphire crystals leads, on the one hand, to the necessity of increasing the number of transits in the active medium and on the other, reduces the ASE level.

## References

1. Agranat M.B., Ashitkov S.I., Ivanov A.A., Konyashchenko A.V., Ovchinnikov A.V., Fortov V.E. *Kvantovaya Elektron.*, **34**, 506 (2004) [*Quantum Electron.*, **34**, 506 (2004)].
2. Pessot M., Squier J., Mourou G. *Opt. Lett.*, **14**, 797 (1989).
3. Strikland D., Mourou G. *Opt. Commun.*, **56**, 219 (1985).
4. Agranat M.B., Ashitkov S.I., Ivanov A.A., Konyashchenko A.V., Ovchinnikov A.V., Podshivalov A.A. *Kvantovaya Elektron.*, **34**, 1018 (2004) [*Quantum Electron.*, **34**, 1018 (2004)].
5. Shcheslavskiy V., Noak F., Petrov V., Zhavoronkov N. *Appl. Opt.*, **38**, 3294 (1999).
6. Togashi T., Nabekawa Y., Sekikawa T., Watanabe S. *Appl. Phys. B*, **68**, 169 (1999).
7. Yakovlev V.V., Ivanov A.A., Shcheslavskiy V. *Appl. Phys. B*, **74**, 145 (2002).
8. Yanovsky V., Felix C., Mourou G. *Appl. Phys. B*, **74**, 181 (2002).
9. Kryukov P.G. *Kvantovaya Elektron.*, **31**, 95 (2001) [*Quantum Electron.*, **31**, 95 (2001)].
10. Agranat M.B., Ashitkov S.I., Ovchinnikov A.V. Patent No. 47140 for a useful model, dated 10.08.05. Priority from 10.03.05.
11. Hentschel M., Uemura S., Cheng Z., Sartania S., Tempea G., Spielmann Ch., Krausz F. *Appl. Phys. B*, **68**, 145 (1999).

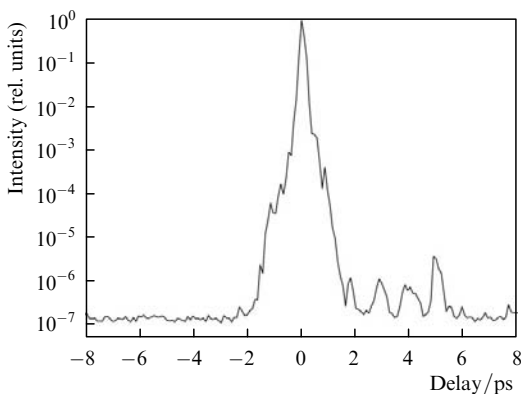


**Figure 10.** Third-order cross-correlation function of the output pulse of the system.